The ITC filter for improving ERS SAR interferograms.

John L. van Genderen, Yonghong Huang,

Rüdiger Gens, Boudewijn S. van Veen and Gerrit Huurneman.

International Institute for aerospace Survey and Earth Sciences (ITC).

P.O. Box 6, 7500 AA Enschede, The Netherlands.

Tel. ++31-53-48 74 254 Fax. ++31-53-48 74 482.

E-mail. Genderen@itc.nl or vveen@itc.nl.

Abstract.

Data from SAR systems can provide information in 3D by using complex radar data, consisting of phase and magnitude components. There are several factors that form an obstacle for achieving high accurate topographic mapping from the interferograms by two dimensional phase unwrapping. One of these factors is the noise in the interferogram, due to decorrelation in data from the different dates. ITC has used existing SAR filters to reduce this noise in interferograms, while preserving the derived phase information. The best results were obtained using speckle reduction by multi-look processing. Also the box filter, tested on raw data was found to be efficient for speckle and noise reduction. This paper describes the first results of applying this new speckle reduction filter to improving the quality of SAR interferograms. The ITC SAR filter design is based upon the MMSE principle and on local area statistics. Furthermore it considers the correlation between filtered pixel and its neighboring pixels. The filter window used, adapts to the image resolution and second order statistics from the central pixel and its neighbors are used to obtain a maximum filter result. The paper will explain the filter and shows the improvements obtained on interferograms.

Introduction

DEM's and land deformation data obtained by interferometric SAR (INSAR) techniques have gained increasing interest from scientists in a variety of research areas, such as geology, hydrology, geophysics, and so on, due to the fact that these products can be created by SAR interferometry from data that can be acquired under all weather conditions in an automatic processing. The SAR interferometric technique combines two complex images recorded with two antennas separated spatially or with one antenna separated in time. The phase and magnitude information of the two complex images is used to produce an interferogram, this is done by multiplying one SAR image with the complex conjugated of the other SAR image. After removing the flat earth phase from the interferogram and solving the 2-D phase ambiguity, a Digital Elevation Map (DEM) can be created. The accuracy of the DEM is strongly influenced by phase noise. If the phase noise is too strong, some fringes will be completely lost which will result in great loss of the accuracy of the DEM. So keeping phase information and removing phase noise in an interferogram is a key point in order to obtain a highly accurate topographic map. One of the major sources of phase noise is decorrelation, which is an inherent property of repeat pass interferometry. If we now assume that the decorrelation depends on the ground cover, we can say that the variance of the phase noise depends on the type of terrain that is being spotted. This assumption makes it possible to apply local adaptive filters (e.g. speckle filters) for reducing the phase noise in interferograms. Speckle arises because the spatial resolution of the sensor is not sufficient to resolve all the individual scatterers. Due to this lack of resolution the resulting complex backscatter of a single resolution cell is the phasor sum of randomly distributed scatterers. It can be shown that the phase of a SAR radar echo, backscattered from a single resolution cell follows a uniform distribution. Speckle is believed to be multiplicactive and can be reduced by averaging independent values with multi-look processing. However, the drawback of multilook processing is that it will result in a loss of spatial resolution since the images used for averaging must be obtained from the same aperture. In order to remedy speckle more efficiently as well as preserving spatial resolution of the images, many speckle filtering techniques have been developed from the image processing field. One of the most representative techniques of speckle reduction in SAR post-processing is the adaptive filtering technique which was first proposed by Lee in 1980. Since then many adaptive filters have been proposed to reduce speckle whilst at the same time preserving the SAR information. However, the full removal of speckle without losing any information is still a long way off. Any filtering technique will more or less damage useful information and leave some residual speckle as it is implemented. The reason for this is that the modern adaptive filters, such as the Lee, Enhanced Lee, Frost, Enhanced Frost, Kuan and Gmap speckle filters, use the local statistical information related to the filtered pixel. The pixel that is filtered is replaced by a value which depends on the statistical information in the filterwindow. This will only result in efficient speckle removal and information preservation when the filter window covers a homogenous areas. When the filter window for example covers an edge the filtered pixel value is replaced by statistical information from both sides of the edge, or from two different phase/intensity distributions. In 1994 Wilhelm Hagg proposed the EPOS filter which used a variable window size and subwindows to deal with this problem. The basic approach of this filter is to search for the biggest homogenous area around the central pixel and use only the statistical information present in this area to filter the central pixel. The EPOS speckle filter is very efficient for removing speckle whilst preserving edges. However, it is not very computationally efficient. Recently ITC proposed a new adaptive speckle filter (Huang Y.H., et al 1997). It uses a common weighting function as filter kernel which is modified by an edge detector to tackle the problem of using statistical information from unwanted areas. It uses not only the local statistical information related to the central pixel but also that from the central pixels neighborhood in the filter window size. The value of this ITC filter for enhancing ERS SAR images has been clearly demonstrated. This paper shows that this ITC filter is also very useful for improving the sharpness of the fringes in SAR interferograms. Computationally efficient this new ITC filter is much more attractive for commercial application.

The ITC Filter technique.

The proposed ITC speckle filter is a modified version of the existing general adaptive filters. We proposed a SINC function as the filter weighting function. The SINC function is coincident to the pulse response function of the SAR system and is therefore more suitable to maintain the radiometric information of the original image as well achieving a low side lobe effect. Additionally, we introduce a new structure in which a non-symmetric change of the filter weighting function can be made. A non- symmetric filter weighting function will, in some cases, preserve radiometric information better than symmetric filters. The thresholds, used by speckle filters to distinguish between homogenous areas and heterogeneous areas, are obtained from the speckle index map of the original image.

A filtered image is the result of the convolution of the original image array, including speckle, with the filter weighting function.

$$G(x,y) = I*W = \sum_i \sum_j I(x+i, y+j) \cdot W(i,j) \qquad \text{[eq. 1]}$$

Where G(x,y) is the filtered pixel value, of a pixel with image coordinates (x,y) in the filtered image array, I(x,y) is a pixel value in the original image array and W(i,j) is the value of a point, with the coordinates (i,j) in the digitized weighting function. According to the impulse response function of a SAR system, the SINC function is chosen as the weighting function,

$$W(i,j)=\frac{\sin\left(K_R\cdot\alpha\cdot\pi\cdot\delta_R\cdot\frac{i}{d_R}\right)}{K_R\cdot\alpha\cdot\pi\cdot\delta_R\cdot\frac{i}{d_R}}\cdot\frac{\sin\left(K_A\cdot\alpha\cdot\pi\cdot\delta_A\cdot\frac{j}{d_A}\right)}{K_A\cdot\alpha\cdot\pi\cdot\delta_A\cdot\frac{j}{d_A}}\cdot C'(i,j) \qquad \text{[eq. 2]}$$

Where K_R, K_A are constants controlling the damping rate of the weighting function, $_{R,A}$ are the range- and azimuth resolution respectively, d_R,d_A are the pixel space of the SAR image in range and azimuth direction respectively, C'(i,j) is an array consisting of zero's and ones used to modify the SINC function according to the local image characteristics present in the filter window, and is the adaptive factor which is expressed as,

$$\alpha=\begin{cases}\dfrac{C_{0,0}-C_{\min}}{C_{\max}-C_{\min}} & \Leftrightarrow C_{0,0}>C_{\min}\\ 0 & \Leftrightarrow C_{0,0}\le C_{\min}\end{cases} \qquad \text{[eq. 3]}$$

Where C_{min} and C_{max} are thresholds used to distinguish between homogenous areas, edges and point targets, and $C_{0,0}$ is the speckle index of the central pixel in the filter window I(x, y). The speckle index is the ratio of the local standard deviation over the local mean in the filter window.

$$C_{0,0}=\frac{\sigma_{local}}{\mu_{local}} \qquad \text{[eq. 4]}$$

Where $\cdot_{local}$ is the standard deviation, and $_{local}$ is the mean of the pixel values within the filterwindow related to the central pixel of the filter window. The weighting function of the ITC filter is modified by C'(i,j), which is expressed as,

$$C'(i,j)=\begin{cases}1\Leftrightarrow & \left|C(i,j)-C_{0,0}\right|\le\sigma_c\\ 0\Leftrightarrow & other\end{cases} \qquad \text{[eq. 5]}$$

Where C(i,j) is the speckle index map of the original image, and $_c$ is determined from calculating the variance of C(i,j). The elements of the speckle index map C(i,j), is the speckle index related to a pixel inside the filter window with coordinates (i,j). To calculate C'(i,j), the speckle index map of the original image has to be calculated before the weighting function can be applied on the image. The window size used to calculate the speckle index of each individual pixel will in most cases equal the size of the weighting function. This implies that pixel values outside the actual filter window of the weighting function are used to modify the weighting function. Actually, C'(i,j) can be modified by the use of different edge detectors, such as the Ratio detector, the Gradient detector, etc. The thresholds C_{max} and C_{min} of the ITC filter are obtained from the speckle index map C(i,j). In order to obtain a reliable estimation of the speckle index distribution a large window (e.g. 65 by 65) is used to calculate the local mean ($_C$)$_l$ and standard deviation ($_{C'}$) of the pixel values inside the window. For every pixel $_{C'}$ and $_{C'}$are used to determine the thresholds which can be expressed as,

$$C_{min} = {}_{C'} \qquad \text{[eq. 6]}$$

$$C_{max} = {}_{C} + {}_{C'} \qquad \text{[eq. 7]}$$

Where is a constant used to adjust the upper threshold, normally with a value in between 1 and 2.

So when filtering a SAR image, every pixel value in the SAR image will be replaced by a new value, which is determined by the following processing steps.

The index map is created by calculating the local speckle index, $\frac{\sigma_c}{\mu_c}$ for every pixel in the image using a selectable window size (usually 5 by 5 or 7 by 7). C(i,j) is an array of values with almost the same dimensions as the SAR image and it will highlight the edges in the SAR image.
The thresholds C_{min}, C_{max} and $_c$ are calculated using the statistical values of a window of C(i,j) which is centered in the pixel that is filtered. The dimension of the window are usually large, e.g. 65 by 65.
C'(i,j) is formed using C(i,j) and $_c$. C'(i,j) is an array consisted of zeros and ones with the same dimensions as the weighting function used to modify the shape of the weighting function.
The adaptive factor is calculated using $C_{0,0}$, C_{min} and C_{max}. The value of increases as $C_{0,0}$ increases, this usually happens when the filter window is covering an edge or point target.
The weighting function is formed using , C'(i,j) and the constants K_R,K_A,$_{R}$,$_{A}$,d_R and d_A.
The central pixel is filtered by means of the convolution of the weighting function with the pixel values within the filter window.
Step II to VI are repeated for every pixel in the original image.

Experimental procedure and results.

INSAR processing can be divided into several steps, which are shown in the flowchart of figure 1.

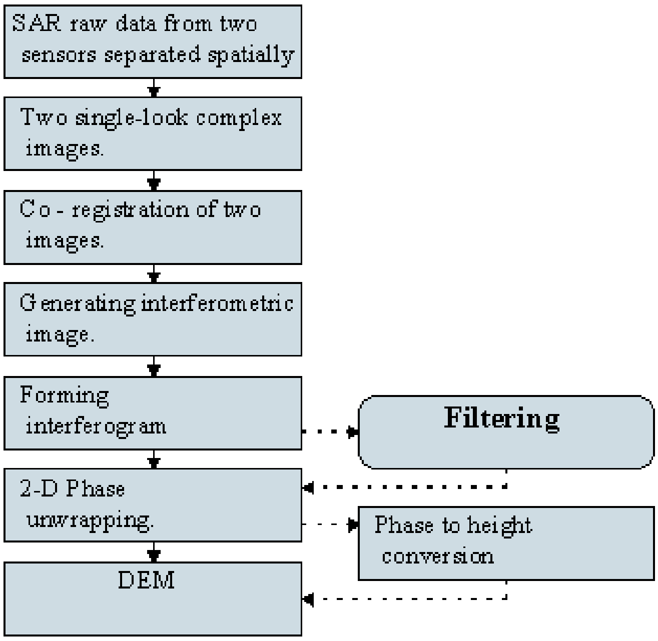

Figure 1 - A flowchart of INSAR processing including filtering.

For the present we have selected to apply the ITC filter just before the 2-D Phase unwrapping, for testing the noise reduction results. In order to avoid the problem of precise registration of the two SAR images, a model is established under the assumption of a airborne repeat path case and an across-track INSAR system. The phase noise due to the decorrelation of a real pair of SAR images, is assumed to be of a Gaussian distribution. The following simulation parameters are included in the model:

Flying height: 3000m

Incident angle: 35

Baseline length 2.0 m

Wavelength` 0.03 m

Terrain model Pyramid

Range sampling points 64

Range resolution 2.0 m

Azimuth Sampling points 64

Azimuth resolution 4.0 m

Phase noise model Gaussian distribution, = 0.0, = 1.0

Thermal noise model Gaussian distribution, = 0.0, = 0.2

SNR 7 dB

Figure 2a shows the simulation result, an interferogram of a pyramid terrain model contaminated by noise. Figure 2b shows a surface plot of a subwindow of figure 2a, which is indicated with a white rectangle in figure 2b.

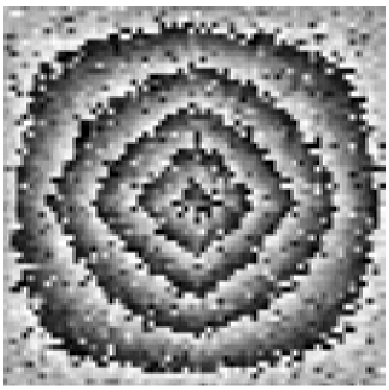

Figure 2a - Interefrogram with noise.

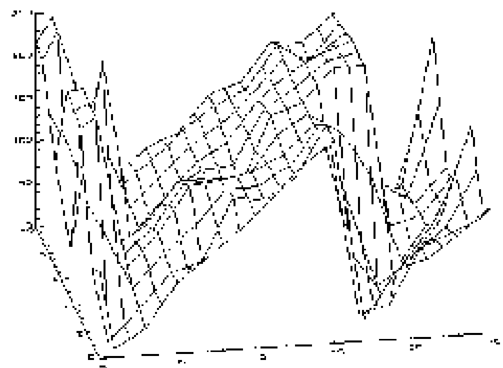

Figure 2b - Surface plot of a subwindow of figure 2a, indicated in that figure with a white rectangle. The horizontal plane represents the pixel positions and the vertical ax the pixel value in the interferogram.

For comparison purposes the interferogram of figure 2a was also filtered using a Lee filter with a window size of 3 by 3. The result of this filtering is illustrated in figure 3. The interferogram filtered with the ITC filter is shown in figure 4. A 3 by 3 window size was used for the weighting function as well as for calculating C(i,j). The thresholds were calculated using the whole image, this was done because of the dimensions of the image (134 by 134 pixels)

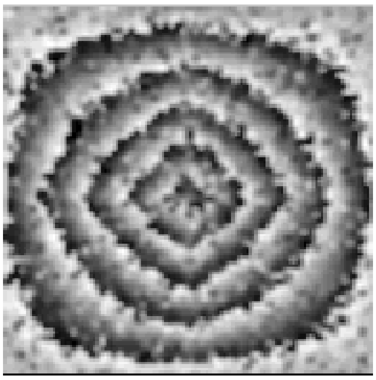

Figure 3a - Interferogram filtered using a Lee Speckle filter with a 3 by 3 windowsize.

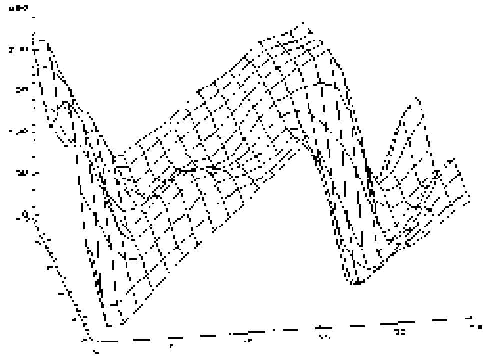

Figure 3b - Surface plot of a subwindow of figure 3a, indicated in that figure with a white rectangle.

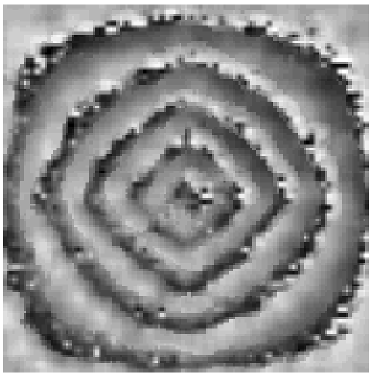

Figure 4a - Interferogram filtered using the ITC Speckle filter, using a 3 by 3 windowsize for calculating the weighting function and c(i.j).

Figure 4b - Surface plot of a subwindow of figure 4a, indicated in that figure with a white rectangle.

Conclusions

When comparing figure 3a with figure 4a we first notice that the interferogram filtered with the ITC filter is less blurred than the interferogram filtered with the Lee filter, this implies than high frequencies are preserved better when using the ITC filter. Noise however is often related to high frequencies but, the "homogenous" parts of the fringes show less phase noise when using the ITC filter then when using the Lee filter. The edges of the fringes however show up sharper, but still contaminated with phase noise, in the interferogram filtered by the Lee filter.

Looking at the results the proposed ITC filter can be a very good solution for the Phase noise problem in interferograms. Future research on the ITC filter with respect to the phase noise reduction in interferograms has good potentials for improving the accuracy of DEM's. The computationally efficient subwindow approach and the usage of second order statistics applied in the ITC filter seem to be promising techniques for reducing phase noise in interferograms.

References.

[1] Yonghong Huang and J.L. van Genderen, "The ITC Filter: a new adaptive filter for SAR speckle reduction", Proceedings of the second International Airborne Remote sensing Conference and Exhibition, vol III, pp 278-287.

[2] Yonghong Huang and J.L. van Genderen, "Speckle and Thermal Noise reduction Techniques for SAR Interferogram".

[3] Yonghong Huang and J.L. van Genderen, " Comarison of several multi-look processing procedures in INSAR processing for ERS-1&2 tandem mode", Proceedings of the Fringe'96 ESA workshop.

[4] R.M.Goldstein, H.A.Zebker and C.L.Werner, " Satellite Radar Interefrometric: Two dimensional phase unwrapping", Radio Sci, Volume 23, No.4, July, 1988, pp 713-720.

[5] F.K.Li, R.M.Goldstein, "Studies of multibaseline Spaceborne Interferometric SAR", IEEE Transac. On Geosci and Remote Sensing, Vol.28, No.1, Jan.1990, pp 88-97.

[6] H.A. Zebker and J. Villasenor, "Decorrelation in Interferometric Radar Echoes", IEEE Transac. On Geosci. and remote Sensing, Vol.3, No.30, Sept.1992, pp.950-959.

[7] D.Massonnet and T.Rabaute, "Radar Interferometry: Limit and Potential", IEEE Transac. on Geosci. and Remote Sensing, Vol.31, No.2, March 1993, pp 455-464.